The scales of the leading-edge separation bubble

The scales of the leading-edge separation bubble

J. A. Smith,[1] G. Pisetta,[1] and I. M. Viola[1, a)]
School of Engineering, Institute for Energy Systems, University of Edinburgh, Edinburgh, EH9 3FB, UK

(Dated: 2 March 2021)

The leading-edge separation bubble (LESB) is a flow feature occurring on the suction side of thin foils as a result of separation at the sharp leading-edge followed by reattachment downstream along the chord. For a flat plate at zero angle of attack, the reattachment length of the bubble depends on the plate thickness t. At a non-zero incidence, instead, the underlying scale governing bubble length is not clear. To investigate, we undertake a critical review of experimental and theoretical studies, and we develop an analytical formulation to predict the reattachment length of plates both at zero and at small incidences. We focus on conditions where the bubble is turbulent, i.e. when transition occurs at a negligible distance from the point of separation. This occurs at thickness- and chord-based Reynolds numbers $Re_t \gtrsim 10^4$, $Re_c \gtrsim 10^5$. At angle of attack $\alpha = 0$, we find that the reattachment length is $x_R \approx 4.8t$ when the chord-to-thickness ratio is $c/t > 12$. At $\alpha > 0$, we find that $x_R/c = \pi\sigma\alpha^2$, where $\sigma \approx 7.9$ is the inverse of the growth rate of a turbulent free shear layer. These results allow estimating x_R on the thin wings of, for example, aerial vehicles and yacht sails.

I. INTRODUCTION

The leading-edge separation bubble (LESB) is a flow feature that occurs on wings, blades, and sails when the leading-edge (LE) is sharp, promoting flow separation, and the angle of attack is sufficiently small to enable reattachment. For example, consider a thin foil at a non zero incidence to a free stream velocity (Fig. 1). An attached boundary layer develops from the stagnation point, which is located on the pressure side, towards both sides of the foil. The flow is driven towards upstream (left in Fig. 1) by the strong suction at the LE, but then it separates due to the adverse pressure gradient as it passes the pressure minimum. At sufficiently small angles of attack, the flow is observed to reattach further aft the foil surface. Reattachment results in recirculation flow towards the LE. The enclosed region of separated flow is the LESB. This paper aims to identify a predictive model of the reattachment length x_R, which is the distance between the point of separation and that of reattachment (Fig. 1).

The pioneering studies on separation bubbles were reviewed by Tani[1] in 1964. Most of the studies focused on the *short laminar separation bubble*, which typically occurs along the suction side of thin foils at moderate Reynolds numbers.[2] The separated shear layer is mostly laminar and reattachment follows shortly after the laminar-to-turbulent transition occurs. Conversely, the LESB discussed in this paper is generated at sharp leading-edges and it is also known as the *long bubble*.[3] In contrast to the short bubble, the shear layer is typically turbulent for most of the bubble length and it has an overall lower impact on the pressure distribution. As pointed out by Castro & Haque,[4] the LESB presents similarities with a wide range of other flow features where a recirculating flow region is bounded between a solid boundary and a turbulent shear layer. These include, for example, the recirculating flow behind a backward-facing step[5] and above a forward-facing blunt plate.[6,7]

a)Electronic mail: i.m.viola@ed.ac.uk.; https://voilab.eng.ed.ac.uk.

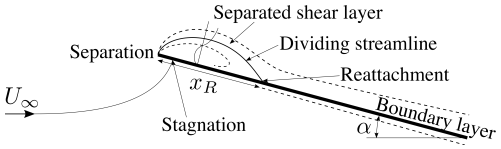

FIG. 1: LESB over a foil with a sharp leading-edge.

The rest of the paper is organised as follows. In Sec. II, we review the reattachment length for a flat plate at zero incidence and with a blunt leading-edge. We will note how the reattachment length becomes independent of the Reynolds number (Sec. II A) and the chord to thickness ratio (Sec. II B) as these increase. In Sec. III we propose a new reattachment length model that shows good agreement with the experimental data.

In Sec. IV we consider a flat plate at incidence. Firstly (Sec. IV A), we review past experiments showing that the reattachment length tends to become independent of the Reynolds number as this increases, but it strongly depends on the angle of attack. Then (Sec. IV B) we review the reattachment model proposed by Newman & Tse.[8] Finally, in Sec. V, we proposed a new reattachment length model that builds from that of Newman & Tse but that shows a much closer fit with the experimental data. Conclusions are drawn in Sec. VII.

II. REVIEW OF THE REATTACHMENT LENGTH OF A FLAT PLATE WITH A BLUNT LEADING-EDGE

We first consider the governing scales of a LESB that occurs on a canonical flow for which experimental data is abundant: the flat plate of finite thickness at zero angle of attack ($\alpha = 0$), i.e. a forward-facing blunt plate (Fig. 2). This flow is effectively an isolation of the leading-edge region of a wing with a blunt LE, with stagnation point on the camber line edge. Ota and co-workers[9–11] and Lane & Loehrke[12] generated significant experimental data between 1970 and 1980 while investigating the heat transfer properties of the flat plate. Dif-

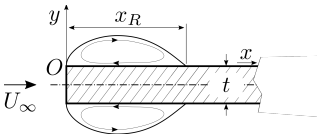

FIG. 2: LESB over a flat plate with a blunt leading-edge.

ferently from a generic forward-facing step, we focus on the conditions where the close proximity between the stagnation and the separation points, $t/2$ in Fig. 2, results in negligible boundary layer thickness at the separation point. The effect of the boundary layer thickness will be discussed in Sec. III.

A. Thickness and Reynolds number

The experimental results from Ota et al.[10] were obtained for thickness Reynolds numbers $40 < Re_t < 2000$ and were combined with further results in 1981 for $2.1 \times 10^4 < Re_t < 6.67 \times 10^4$. Lane & Loehrke[12] carried out similar work, varying Re_t as well as the chord and thickness of the plate. A comparison of the results obtained in this research, together with the more recent numerical results from Tafti & Vanka,[13] is given in Fig. 3a. The collapse of the data confirms the thickness as an appropriate length scale for the reattachment length.

It is instructive to compare the trend of the reattachment length with Reynolds number against that of backward-facing step. This is shown in Fig. 3b, which reports the data measured by Back et al.[14] Here, the reattachment length is nondimensionalised by the step height h, which is also used to define the Reynolds number Re_h. Focusing on the low Re range ($Re_t < 400$), we may make direct comparison between the flat plate and the backward-facing step. Qualitatively, a comparison between Fig. 3a and 3b shows a noticeably similar trend of x_R with the Reynolds number.

Discussion by Ota and colleagues suggests that the laminar or turbulent state of the separated shear layer (SSL) is the governing factor for reattachment length x_R. Despite the different values of chord-to-thickness ratio c/t shown in Fig. 3a, reattachment lengths agree in the laminar region once nondimensionalised by thickness, t. This suggests that x_R is chord-length independent for the range of c/t reported. A peak in x_R occurs where the SSL becomes transitional, oscillating between turbulent and laminar prior to turbulent reattachment. In this case, we observe peak $x_R \approx 7t$ at $Re_t \approx 300$ for all values of c/t investigated. In shorter plates ($c < 7t$), Lane & Loehrke[12] note x_R is constrained by plate length, with separated region spanning the entire chord at low Re.

For higher Reynolds number conditions, Ota et al.[11] report an undulating lateral motion of the SSL that grows in extent with increasing Re_t. This is consistent with observations

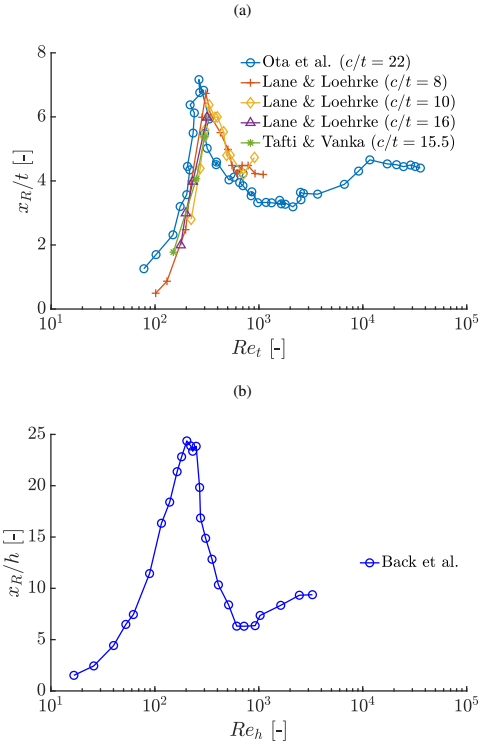

FIG. 3: Variation of the nondimensionalised reattachment length x_R/t and x_R/h with Reynolds number Re_t and Re_h for (a) a plate with a blunt leading-edge and (b) a backward-facing step, respectively.

of the aforementioned backwards-facing step.[14,15] As Re_t increases further, beyond approx. 10^3, the spread of the SSL steadies. Gartshore & Djilali[16] postulate that full turbulence is not achieved until $Re_t > 2 \times 10^4$. From Fig. 3a and 3b we observe x_R steadies to an approximately constant value once this threshold is reached. Here we infer Reynolds number independence is reached, implying that there exists a critical Reynolds number at which further increase has negligible effect on the flow behaviour.

The similarities between the trends of the reattachment length with t and h for the plate with a blunt leading-edge and the backward-facing step confirm that the governing reattachment mechanism is also similar.[4] The key difference between the two flow conditions is the development of the upstream boundary layer. This has been shown by Westphal et al.[17] to heavily influence reattachment length. Desire to limit boundary layer development inspired much of the work of Ota and his associates, and we have noted its effect on reattachment length even in the context of the flat plate provided $Re_t \lesssim 400$.

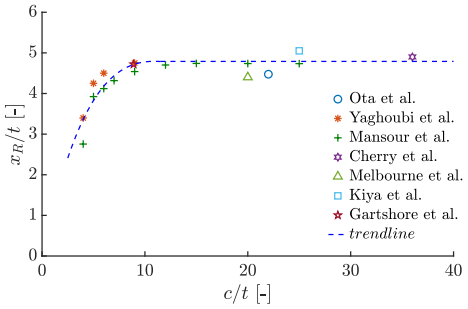

FIG. 4: Variation of thickness-nondimensionalised reattachment length x_R/t with chord length c/t for a plate with a blunt leading-edge. Data replotted from various works (see legend).

Another influence present only in the backward-facing step flow regime is the channel expansion ratio. Studies undertaken by Ötügen[18] found this had measurable effects on reattachment length.

B. Chord-to-thickness ratio

Experimental studies of the turbulent properties of the reattaching zone by Kiya & Sasaki,[19] Cherry & Hillier[20] and Gartshore & Djilali,[16] take place at higher Re_t within the fully turbulent SSL region. Additionally, Yaghoubi & Mahmoudi[21] and Mansour & Hosseinverdi[22] developed more recent numerical models varying c/t at high Re_t. These studies concur that increasing Re_t has negligible effect on x_R/t at this range, in support of Ota's earlier observations.

Importantly, we observe a clear trend between x_R/t and c/t: shorter plates appear to have notably lower thickness-nondimensionalised reattachment lengths than longer ones, with x_R/t variation with c/t ceasing beyond a critical value of the latter. Figure 4 outlines this trend, illustrating a limiting value of x_R/t is reached for $c \gtrsim 12t$. Once this limit is reached, $x_R \approx 4.8t$. Although good agreement is observed between the numerical studies of Yaghoubi[21] and Mansour,[22] there are some variations in the experimental results. Some of these discrepancies may be explained by variation in experimental method and conditions. For example, Saathoff & Melbourne[23] explored the peak pressure generation in the flow and varied freestream turbulence intensity T_u. Elevating T_u has been shown to decrease reattachment length due to increased mixing and entrainment of the SSL,[16,23,24] and therefore lower x_R may be expected. Kiya et al.[25] report a marginally higher x_R than expected, however it is noted that end plates were not fitted for their wind tunnel experiment. These fixtures are important when analysing nominally two-dimensional flows and could contribute to the mild deviation in results.[26,27] Taking these factors into consideration, it appears the trend holds validity.

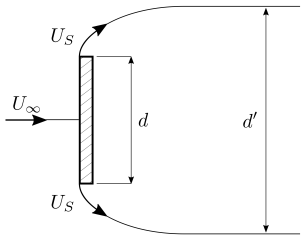

FIG. 5: Schematic drawing of the free streamline of a plate at $\pi/2$ incidence.[29]

III. A NEW REATTACHMENT LENGTH MODEL FOR A FLAT PLATE WITH A BLUNT LEADING-EDGE

Kirchhoff[28] developed the concept of the *free streamline*, which enables the overcoming of d'Alembert's paradox of zero drag in potential flow. He considered a flat plane normal to the stream, as pictured in Fig. 5. At the sharp edge of the plate, a separated shear layer is formed and it carries the majority of the vorticity formed at the plate. Kirchhoff separated the fluid domain into an outer potential-flow region, where viscosity is negligible, and a wake region containing the vorticity generated at the solid boundary and shed into the wake. Noting that the pressure is about constant on the downstream side of the plate, he modelled it as a constant *base pressure* equal to the free stream pressure.

Roshko[29] further developed this theory noting that a lower base pressure than the free stream pressure is needed to achieve good agreement with experimental data. This is equivalent to setting the velocity along the free streamline in the near wake at $U_s > U_\infty$. In the far wake, the pressure and the velocity approach the free stream values. Hence, Roshko separated the wake into a near wake region, where the base pressure is roughly constant, and the *coupling region*, where vortex shedding or other mixing phenomena occur and the pressure recovers towards the level of the free stream pressure. In the near wake, the free-streamline theory predicts a unique relationship between the nondimensional streamline velocity U_s/U_∞, the nondimensional wake width d'/d, and the plate drag coefficient.[29]

The base pressure shows some variability between different body shapes but it has a mild effect on the free streamline.[29] This prompted us in applying free streamline theory to the flat plate with a blunt leading-edge in Fig. 2. Let us deform the plate in Fig. 5 considered by Kirchhoff and Roshko, by extending indefinitely the horizontal dimension of the plate, such to achieve the blunt plate in Fig. 2. Hence, the thickness t of the plate with a blunt leading-edge is equivalent to the plate height d.

The pressure inside the bubble is about constant in the upstream region of the bubble,[6,16,20] and it is equivalent to Roshko's base pressure. The pressure mildly decreases towards a minimum in the centre of the vortex associated with the LESB, and then increases towards the reattachment point

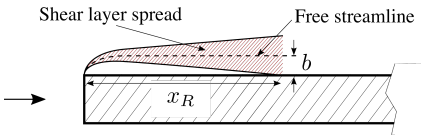

FIG. 6: Schematic drawing of the linear spread rate of a turbulent free shear layer along the free streamline of a plate with a blunt leading-edge resulting in downstream reattachment.

as in Roshko's coupling region. The free streamline is governed by its initial direction at the separation (i.e. orthogonal to the free stream) and the value of the base pressure. We can therefore use free-streamline theory to estimate the bubble height.

As Roshko's data shows, d' varies directly with d and, hence, with t. This trend is concurrent with the present authors' findings presented in Sec. II A, as we would expect a proportional relationship between x_R and free streamline deflection from the separation point since x_R scales with t. A wider deflection of the free streamline results in a longer reattachment length.

Since we know the SSL is turbulent almost immediately after separation,[30] we might assume that the SSL is a turbulent free shear layer (FSL), following the free streamline as a centreline. Let us assume that the initial boundary layer thickness is negligible; we will return to this assumption later. It follows, then, that the point at which reattachment occurs will be the point at which the lowest extent of the FSL velocity profile has spread to an extent b that coincides with the displacement of the free streamline, $(d'-d)/2$; Fig. 6 illustrates this conceptual idea.

Let σ be the inverse growth rate of the lowest streamnormal extent of the turbulent separated shear layer with respect to centreline. The reattachment length can be computed as

$$x_R = \sigma b = \frac{\sigma(d'-d)}{2}. \tag{1}$$

Finally, by taking Roshko's flat plate as Ota's blunt leading-edge, we have $d = t$, and thus the previous equality can be nondimensionalised as

$$\frac{x_R}{t} = \frac{\sigma}{2}\left(\frac{d'}{d} - 1\right). \tag{2}$$

This in an interesting expression that includes terms from the various flows described above: the plate thickness t, the free shear layer inverse spreading rate σ, the free streamline wake width d'/d.

To verify this model, we extract data from studies undertaken into the terms mentioned. Starting with wake width, d'/d, we look to Roshko's research.[29,31] He identified that breaking the communication between the two separated shear layers with a splitter plate has an effect on vortex formation and free streamline displacement. In our case, separation occurs at the leading-edge of the foil, and the remainder of the foil chord extends downstream as Roshko's splitter plate. He presents experimental data for free streamline displacement given a sharp edged normal plate (Fig. 5) with a splitter plate located on the centreline of the wake (see Table 1, row J in Roshko's NACA Technical Note).[31] Of all free streamline data reported, this appears to be the best approximation of our case as illustrated in Fig. 6. For this case, 11 measurements of the wake width yield $1.96 < d'/d < 2.16$, giving $d'/d = 2.06 \pm 0.05\%$.

Numerous studies have been undertaken into the spreading behaviour of the turbulent free shear layer. Birch & Eggers[32] compiled data from 12 studies and asserted that, in a turbulent regime, the dependence on the Reynolds number is very weak for this flow type (see also Nieuwstadt et al.)[33] This similarity in behaviour is quantified by similar observed spreading rates. Champagne et al.[34] compiled spreading data for eight investigations studying the behaviour of a uniform freestream of velocity spreading into quiescent surrounding fluid, charting the rate of divergence between two isolines of velocity at 0.95 and 0.10 of the free stream representing the streamnormal extent of the shear layer. In the present model, we focus on the spreading rate of the low extent of the velocity profile from the centreline of the turbulent free shear layer.

Accounting for the uneven growth distribution of the shear layer, quantified by divergence of its centreline from the splitter plate direction as reported in each of the aforementioned studies,[34] it is found that the range $6.9 < \sigma < 9.1$ applies to 6 of the 8 studies, where the 2 outliers employed a significantly different experimental technique using a trip wire. These 6 studies result in a mean value $\sigma = 7.9 \pm 15\%$.

Research undertaken into the spreading of turbulent jets[35–37] has yielded comparable but slightly higher σ values, with $10.4 < \sigma < 11.6$. This is to be expected as in this flow type the centreline remains in line with the nozzle due the symmetrical parabolic velocity profile upon entry into the quiescent stream, thus the growth rate is evenly distributed between respective streamnormal extents and the centreline.

Returning to our model with the above values, the right hand side of Eq. 2 becomes $x_R/t = 4.2 \pm 15\%$, which is in agreement with our analysis of the experimental findings detailed in Fig. 4, where $x_R/t \approx 4.8$, implying that the growing turbulent shear layer provides an effective model of the LESB's outer shear layer.

Let us now estimate the effect of the thickness of the boundary layer at the separation point, by comparing its magnitude with the thickness of the shear layer at the reattachment point. From Fig. 3a, the reattachment length becomes independent to the Reynolds number for $Re_t > 10^4$. Hence, let us consider this limiting condition, for which the boundary layer thickness

is maximal. The boundary layer develops from the middle of the blunt edge in Fig. 2 and thus the Reynolds number at separation is $Re_t/2 = 5 \times 10^3$. Noting that transition on a boundary layer with zero pressure gradient occurs at around 5×10^5 and that the pressure decreases from the stagnation point to the separation point, the boundary layer is likely to be laminar. Using Blasius solution,[38] we find that the boundary layer thickness is $\delta_{\mathrm{BL}} = 0.035t$. In contrast, the shear layer thickness at the reattachment point is $\delta_{\mathrm{FSL}} = 2x_R/\sigma \approx 0.8t$, which is more than 20 times higher than δ_{BL}. Hence, accounting for the boundary layer thickness as a starting thickness of the shear layer at separation would result in less than a 5% change in the estimate of the reattachment length.

IV. REVIEW OF THE REATTACHMENT LENGTH OF A FLAT PLATE AT INCIDENCE

A. Angle of Attack and Reynolds Number

Crompton & Barrett[30] undertook extensive investigation into the sharp-edged plate at incidence. They reported reattachment lengths over a range of velocities at different α. The plate used had $c/t = 26.7$, and as such we would expect the effect of further increasing chord-length on the results to be negligible at $\alpha = 0$. As we will demonstrate in this section, however, for angles of attack different from zero and high c/t, the governing length scale is the chord length. Hence, in Fig. 7, we plot their results in terms of Re_c and we find good agreement with the conclusions drawn in Sec. II A.

For $\alpha \geq 5^\circ$, leading-edge stall is reported. At $\alpha = 1^\circ$, $x_R \approx 4t$. This is comparable to that observed on the flat plate at $\alpha = 0$, however perhaps slightly lower than we expect (Fig. 7). Nevertheless, Fig. 7 shows that x_R is clearly highly sensitive to changes in α. Finally, the authors report that for all α tested, the stagnation point remained fixed very close to the leading-edge.[39] As we observe in Fig. 7, for $Re_c \gtrsim 2 \times 10^5$, the effect of this small distance between stagnation and separation is that upstream boundary layer development is negligible and no longer influences reattachment length.

Reynolds independence is reached at $Re_c \geq 10^5$, which is equivalent to $Re_t \gtrsim 10^4$. The SSL has been shown to transition to fully developed turbulence almost immediately after separation at moderate to high Reynolds number regimes. Gault,[40] for example, found that, on foils with a sharp LE, transition occurs at a Reynolds number based on the distance from the LE, $Re_x \approx 5000$. Fig. 8 plots the turbulence intensity of the SSL generated over the sharp plate at incidence investigated by Crompton & Barrett.[39] The scale bar indicates the magnitude of the root mean square of the velocity u_{RMS} relative to the freestream velocity U_∞. For this specific condition, the plot indicates that full turbulent transition occurs at a chordwise coordinate from the LE, $x \approx 0.02c$. The chord-based Reynolds number is $Re_c = 2.13 \times 10^5$ and thus $Re_x \approx 4000$, which is consistent with the findings of Gault.[40] This example shows how transition occurs at the very beginning of the LESB, in fact the reattachment occurs at $x_R \approx 0.5c$. This early transition in the LESB is corroborated by several other experimental studies.[8,40,41]

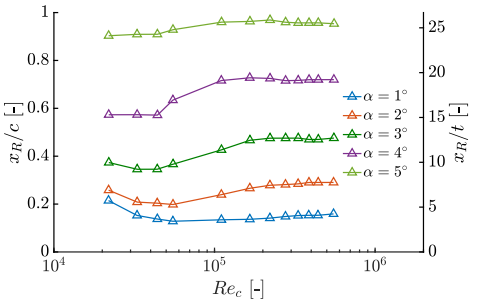

FIG. 7: Chord-nondimensionalised reattachment lengths across a range of chord-based Reynolds number Re_c and angle of attack α (Crompton & Barrett).[39]

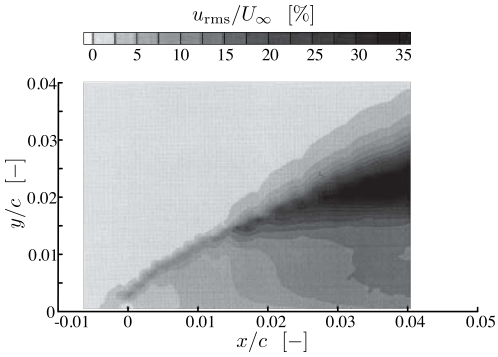

FIG. 8: Laminar-to-turbulent transition of the LESB separated shear layer at $Re_c = 2.13 \times 10^5$, $\alpha = 3^\circ$ (edited from Crompton & Barrett).[39]

B. The Reattachment Length Model of Newman and Tse, 1992

In the case of the LESB, as discussed in Sec. II A, we know that there is negligible boundary layer development upstream of separation once a fully turbulent SSL Re value is reached and reattachment length becomes independent of Re. Let us consider the displacement thickness, δ_1, of the SSL at reattachment. Conceptually, δ_1 is a length by which an equivalent freestream with no shear flow would be displaced. Unfortunately, δ_1 measurement at x_R requires complex experimental procedure, and the results could be unreliable due to the unsteady nature of the reattachment location.[42] Newman & Tse[8] navigated this problem by noting that by considering the drag of the bubble alone, in the far wake the displacement and mo-

mentum thicknesses should equate: $\delta_1 = \delta_2$. We will now follow in detail the derivations of Newman & Tse[8] because, in Sec. V, we will review their approach to develop a new model that seems to provide a better fit with the experimental data.

We may obtain δ_2 analytically from the drag induced by the bubble using the known relationship between drag and momentum thickness,

$$D = \rho U_\infty^2 \delta_2. \tag{3}$$

Assuming negligible camber, thin aerofoil theory gives the chord-normal force coefficient for a thin foil as

$$C_F = 2\pi \sin\alpha \approx 2\pi\alpha, \tag{4}$$

and the force

$$F = \frac{1}{2} C_F \rho U_\infty^2 c. \tag{5}$$

The drag is given by

$$D = F \sin\alpha \approx F\alpha. \tag{6}$$

Hence by substituting Eq. 4 in Eq. 5, and the result in Eq. 6, we find:

$$D = \left(\frac{1}{2} C_L \rho U_\infty^2 c\right)\alpha = \left[\frac{1}{2}(2\pi\alpha)\rho U_\infty^2 c\right]\alpha = \pi\rho U_\infty^2 c\alpha^2. \tag{7}$$

To model the flow-displacing effect of the LESB, Newman & Tse[8] proposed an array of potential sources of equal strength spanning x_R. The sources, which have a total strength per unit length m, deliver the volume flux mx_R entrained by the separated mixing layer and shift the freestream upwards by δ_1. This is shown schematically in Fig. 9. From the equivalence of the volume fluxes, $U_\infty\delta_1 = mx_R$, and by assuming $\delta_1 = \delta_2$, it follows that $U_\infty\delta_{2,R} = mx_R$ (where $\delta_{2,R}$ is the value of δ_2 at $x = x_R$). Equating the drag computed in Eq. 7 with the δ_2-based drag definition, we find

$$\pi\rho U_\infty^2 c\alpha^2 = \rho U_\infty^2 \delta_{2,R} = \rho U_\infty m x_R. \tag{8}$$

Considering the equality between the external terms and rearranging for the chord-nondimensionalised reattachment length, we find

$$\frac{x_R}{c} = \frac{U_\infty}{m}\pi\alpha^2 \tag{9}$$

where

$$\frac{U_\infty}{m} = \left(\frac{\delta_2}{x}\right)^{-1} \tag{10}$$

which is about 50 along a FSL. Newman & Tse[8] confirmed experimentally the dependency of the reattachment length with the square of the angle of attack, as predicted by

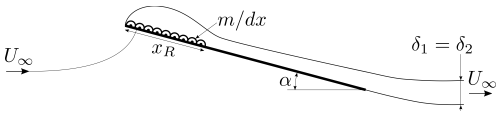

FIG. 9: Schematic drawing of an array of sources with specific strength m mimicking the presence of the LESB and the resulting streamlines around a foil at incidence.[8]

Eq. 9, but found a slope closer to 12π rather than the theoretical 50π.[43] They attributed this divergence to backflow within the bubble and to the pressure rise at reattachment.

To further assess the effectiveness of this model, in Fig. 10 we compare the data from various authors. Fig. 10a shows x_R/c versus α^2, from which we observe an almost linear trend, while Fig. 10b shows the slope $x_R/c\alpha^2$ of the curve. Gault & McCullough,[3] Rose & Altman[44] and Newman & Tse[8] all conducted experiments on the double-wedge foil geometry, reporting reattachment length. Studies into thin foils for turbomachinery applications by Walraevens & Cumpsty,[45] Hazarika & Hirsch,[46] Tain & Cumpsty[47] and Arena & Mueller[48] provide detail on LESB characteristics in this context, although only Arena & Mueller[48] report reattachment length variation with angle of attack on their test geometry. Additionally, research from Ravi[41] in the context of micro aerial vehicles and results from wind tunnel testing on a thin NACA foil from McCullough & Gault[3] are also included for comparison. It is noted that curved leading-edges do not provide as consistent a separation point as sharp-edged foils, however Tain[47] reports separation occurring very near the blend point, where the leading-edge becomes the upper foil surface, in most cases. This means results between these experiments are comparable. Nevertheless, the larger-radius rounded leading-edge provides a less abrupt adverse pressure gradient than the sharp-edge, and as such we might expect to see the LESB develop at a different rate with α. The divergence of the slope from the constant theoretical value, instead, was already observed by Newman & Tse,[8] who, as mentioned, attributed this to the backflow within the bubble and to the pressure rise at the reattachment point. In Fig. 10b we include the model predicted by Newman & Tse[8] alongside the model described in Sec. V.

The linear variance with α^2 appears to hold in all cases across a significant range of α and c/t , including when reattachment occurs near the trailing edge. In contrast, the trend breaks for $\alpha \lesssim 3°$. At low angles of incidence, we infer that

LE geometry (e.g. the thickness t) takes precedence in LESB scale, as in Sec. II and III . Newman & Tse[8] also suggests an increase in viscous effects at lower α gives shorter x_R. While the data in Fig. 10a shows a common almost linear trend with α^2, the slopes and the intercepts vary. Newman & Tse[8] estimated a null intercept and a slope of $\pi x/\delta_2$, which they assumed should be constant for all experiments because they neglected the effect of the thickness. In reality, instead, the intercept depends on the thickness and the leading-edge shape. We identify three outliers, those with high values are Crompton & Barrett[39] who used a 20° chamfer projecting upstream the shear layer, and Arena and Mueller[48] because of the low c/t. The low intercept is the rounded nose of the NACA 64006 tested by Gault & McCullough.[3] The other tests, which all gave an almost null intercept, were performed on sharp wedges with an angle of about 5° made between the upper and lower surfaces of the foil at the leading-edge.

V. A NEW REATTACHMENT LENGTH MODEL FOR A FLAT PLATE AT INCIDENCE

We attempted to incorporate c and α into our model developed in Sec. III. The main challenge is the estimate of the displacement of the free streamline. For $\alpha = 0$, we solved this issue by assuming that the plate thickness t would have played the role of Roshko's plate height d. If we attempted a similar approach by considering, for instance, the frontal projection of the plate, $d = t\cos\alpha + c\sin\alpha$, we would eventually find that the reattachment length grows proportionally to α. We have shown however that both the theoretical analysis of Newman & Tse[8] and the experimental data suggest a quadratic growth with the angle of incidence. We therefore borrow some of the approach proposed by Newman & Tse,[8] by returning to Eq. 8. We consider the first equality between the first two terms, and we rearrange for the momentum thickness, finding $\delta_2 = \pi c\alpha^2$. Most of the drag of a foil with a LESB is due to the bubble. Therefore, we assume δ_2 of the bubble's SSL to grow to the level of $\pi c\alpha^2$, and then to remain about constant within the boundary layer along the remaining length of the foil. We also borrow from Newman & Tse[8] the assumption that the displacement and momentum thicknesses of the SSL are equal, $\delta_1 \approx \delta_2$.

The displacement thickness represents the displacement $b = (d' - d)/2$ of the free streamline, and thus we find the squared relationship with the angle of incidence: $b = \pi c\alpha^2$. If we then adopt the same approach that we used for the zero-incidence case (Sec. III), we assume that reattachment occurs when the growth of the FSL pairs the displacement of the free streamline, and, as before, we conclude that $b = x_R/\sigma$. Therefore, by equating these two estimates for free streamline displacement, and rearranging for the chord-normalised reattachment length, we find

$$\frac{x_R}{c} = \pi\sigma\alpha^2. \tag{11}$$

To test the validity of this model, we plotted the slope $\pi\sigma$ in Fig. 10b. The different experimental results seem to converge consistently towards this slope. It is noted that, if the LESB does not vanish in the limit of $\alpha \to 0$ due to a blunt leading-edge, then $x_R/c\alpha^2 \to \infty$ as observed in Fig. 10b for the data of Crompton & Barrett[39] and Arena and Mueller.[48]

Despite the marked simplicity of the proposed models for $\alpha = 0$ (Eq. 2) and $\alpha > 0$ (Eq. 11), they both seem to provide a relatively accurate estimate of the LESB reattachment length.

VI. DISCUSSION

Similarly to Eq. 1 for $\alpha = 0$, also Eq. 11 shows that the reattachment length x_R depends linearly on the initial displacement of the separated shear layer, which is bt for $\alpha = 0$ and $\delta_2 = \pi c\alpha^2$ for $\alpha > 0$. When $\alpha = 0$, the displacement bt is governed by the direction of the shear layer at the separation point, i.e. orthogonal to the free stream, and by the constant base pressure. Hence, for $\alpha = 0$, the displacement of the shear layer can be computed by knowing the base pressure or assuming the same base pressure of similar geometries, such as a flat plate normal to the stream with a splitter plate in the wake.

For Kirchhoff's plate, normal to the stream, the product of the base pressure with the distance between the two free-streamlines in the wake, is the drag. The total drag can be broken down into a component associated with the plate diameter d, and a component associated with the shear layer displacements $d' - d$. Hence, when in Eq. 1 we assume that that the height of the LESB in Fig. 6 is $b = (d' - d)/2$, we are assuming that the drag associated with the shear layer displacement is the drag of the LESB. We showed, in fact, that this is the same underlying hypothesis of Newman & Tse[8] for a plate at incidence (Sec. IV B).

As the angle of attack increases, the flow is no longer symmetrical and bound circulation is formed. As shown by Yeung & Parkinson,[49] who solved the free streamline problem with a wake-source model,[29] bound circulation must be considered to correctly predict how the free streamline turns towards the plate. Hence, the distance between the free-streamlines in the wake can no longer be taken from that of a flat plate normal to the stream. However, the problem is solved by recalling that we can equivalently estimate the LESB's drag (D) to find the displacement of the shear layer ($b = \delta_2 = D/\rho U^2$).

The reattachment length can be written explicitly as a function of the LESB's drag coefficient $Cd \equiv 2D/(\rho U^2 c)$. From Eq. 8, we find immediately that $Cd = 2\pi\alpha^2$. Hence, our model presented in Eq. 11 can equivalently be written as

$$\frac{x_R}{c} = \frac{Cd}{2}\sigma \tag{12}$$

where Cd is the drag coefficient associated with the LESB.

Finally, our model shows that the reattachment length is proportional to the inverse growth rate of the shear layer, σ. This effect can be isolated for a backward-facing step with height h, where the free streamline can be taken as parallel to the free stream and the first equality of Eq. 1 reduces to

$$\frac{x_R}{h} = \sigma. \tag{13}$$

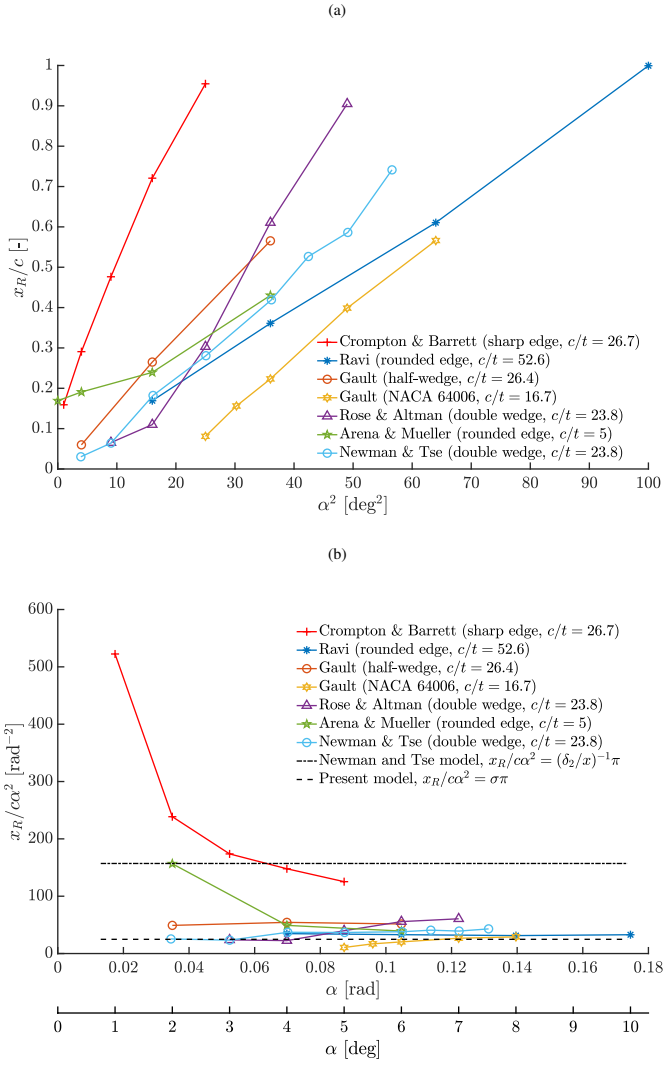

FIG. 10: (a) Chord-nondimensionalised reattachment length x_R/c and, (b) slope of the linear model $x_R/c\alpha^2$, versus the square of the angle of incidence α^2. Data replotted from various works (see legend) and model presented in Sec. V.

By using the range of σ of Champagne et al.[34] as in Sec. III, we find $x_R/h = 7.90 \pm 1.1$. This is in agreement with the experimental data,[5] which suggests that the reattachment length approaches $x_R/h \approx 8$ from lower values as the Reynolds number increases.

The linear relationship between x_R/h and σ also offers useful insights. For example, an akin approach to Eq. 13 was adopted by Yang & Meneveau[50] to estimate the sheltering length of larger roughness elements with size h on smaller downstream elements. They postulated, and verified with numerical simulations, that the sheltering effect would extend downstream up to a nondimensional distance $x_R/h \sim U_c/u_t$, where U_c and u_t are the convective and mixing velocity scales, respectively. As the inverse growth rate σ is the ratio be-

tween the streamwise and streamnormal length scales of the free shear layer, they used the ratio between the streamwise and streamnormal velocity scales.

Overall the proposed model is expected to be resilient to minor variations of the geometry and flow conditions because derived from basic principles. The model, for example, should correctly predict the reattachment length over a cambered sail as long as the chord-normal force in Eq. 4 is corrected for the camber. A limitation of the model as presented, is that the formulations for $\alpha = 0$ and $\alpha > 0$ are based on the two governing length scales t and c, respectively, and thus none of the formulation can be used for those angles of attack where both scales are relevant. The data in Figure 10b suggests that when $c/t \approx 4\%$, the thickness scale becomes negligible at $\alpha > 2^\circ - 6^\circ$. The model does not account for the pressure gradients due to other solid boundaries such as the channel walls, that can either displace the shear layer, or vary its growth rate.

VII. CONCLUSION

We investigate the characteristic length of the turbulent leading-edge bubble, a feature that occurs at the sharp edge of thin wings in moderate and high Reynolds number conditions. We focus on a flat plate at the thickness- and chord-based Reynolds numbers $Re_t \gtrsim 10^4$ and $Re_c \gtrsim 10^5$, respectively. At zero and small angles of attack, a laminar boundary layer separates at the sharp edge, forming a separated shear layer. Transition occurs at a negligible distance from the leading-edge compared to the distance to the reattachment, resulting in a turbulent bubble between the plate and a free shear layer. We found that the reattachment length can be predicted by assuming that the separated shear layer is parallel to the free stream (and, for small angles of attack, also to the plate), and its thickness increases as the same rate as a turbulent free shear layer. Reattachment occurs when the shear layer thickness as measured from centreline to lowest streamnormal extent is equal to the distance between the shear layer centreline and the plate. The challenge is to predict the distance of the shear layer centreline from the plate.

For zero angle of attack, we found a suitable displacement of the shear layer considering Kirchhoff's ideas of the free streamline passing through the edges of a plate orthogonal to the flow. Using experimental data from Roshko[29] for the displacement of the free streamline, and data from Champagne et al.[34] for the growth of the turbulent free shear layer, we found that the reattachment length is $x_R/t = 4.2 \pm 15\%$, where t is the plate thickness. This model is in agreement with a review of the experimental data, which suggest that $x_R/t \approx 4.8$ when the chord-to-thickness ratio $c/t > 12$.

At non-zero angles of attack, the free streamline approach does not hold. Inspired by the work of Newman & Tse,[8] we found a suitable displacement of the shear layer recalling that the displacement thickness is proportional to the drag, which is the streamwise projection of the wall normal force associated with the plate's circulation. This analysis results in the simple formula $x_R/c = \pi\sigma\alpha^2$, where $\sigma \approx 7.9$ is the inverse of the growth rate of a turbulent free shear layer, and α is the angle of attack. We verified this result against a wide range of experiments and found a step increased agreement from the model of Newman & Tse.[8]

These two formulations, $x_R/t \approx 4.8$ and $x_R/c = \pi\sigma\alpha^2$, provide the relationship between the leading-edge bubble length and the governing length scale, which is the plate thickness t at low angles of attack ($\alpha \to 0$) and the chord c at non-zero angles of attack. These can be used to estimate the reattachment length of wings with a sharp leading-edge such as, for example, yacht sails and the thin wings of micro aerial vehicles. The latter wings typically have a low camber and can operate over a range of angles of attack near the stall angle. Because stall occurs when the reattachment length is greater than the chord, it is plausible that these formulations could help in predicting when stall might occur.

AUTHOR'S CONTRIBUTIONS

The study was led by JAS under the supervision of IMV and GP. JAS developed the zero angle of attack formulation whilst IMV developed the small angles of attack formulation. JAS and IMV equally contributed to the writing of the manuscript.

ACKNOWLEDGMENTS

This work received funds from the UK Engineering and Physical Sciences Research Council (EPSRC) via the EPSRC Centre for Doctoral Training in Wind and Marine Energy Systems (EP/L016680/1).

DATA AVAILABILITY

Data sharing is not applicable to this article as no new data were created or analysed in this study.

REFERENCES

[1]I. Tani, "Low-Speed Flows Involving Bubble Separations." Prog. Aeronaut. Sci. **5**, 70–103 (1964).
[2]D. E. Gault, "Boundary-Layer and Stalling Characteristics of the NACA 63-009 Airfoil Section," Natl. Advis. Commetee Aeronaut. Tech. Note No. 1894 (1949).
[3]G. McCullough and D. E. Gault, "Examples of Three Representative Types of Airfoil-Section Stall at Low Speed," Tech. Rep. (1951).
[4]I. P. Castro and A. Haque, "The structure of a turbulent shear layer bounding a separation region," Journal of Fluid Mechanics **179**, 439–468 (1987).
[5]B. F. Armaly, F. Durst, J. C. F. Pereira, and B. Schönung, "Experimental and theoretical investigation of backward-facing step flow," J. Fluid Mech. **127**, 473–496 (1983).
[6]N. J. Cherry, R. Hillier, and M. E. Latour, "The unsteady structure of two-dimensional separated-and-reattaching flows," J. Wind Eng. Ind. Aerodyn. **11**, 95–105 (1983).
[7]L. Hung, P. Moin, and J. Kim, "Direct numerical simulation of turbulent flow over a backward-facing step," J. Fluid Mech. **330**, 349–374 (1997).
[8]B. G. Newman and M. Tse, "Incompressible Flow Past a Flat Plate Aerofoil with Leading Edge Separation Bubble," Aeronautical Journal **96**, 57–64 (1992).

[9]T. Ota and N. Kon, "Heat transfer in the separated and reattached flow on a blunt flat plate," Journal of Heat Transfer **96**, 459–462 (1974).
[10]T. Ota and M. Itasaka, "A Separated and Reattached Flow on a Blunt Flat Plate," American Society of Mechanical Engineers (Paper) **98**, 79–84 (1975).
[11]T. Ota, Y. Asano, and J. Okawa, "Reattachment length and transition of the separated flow over blunt flat plates." Bulletin of the JSME **24**, 941–947 (1981).
[12]J. C. Lane and R. I. Loehrke, "Leading Edge Separation From a Blunt Plate At Low Reynolds Number." American Society of Mechanical Engineers, Heat Transfer Division, (Publication) HTD **13**, 45–48 (1980).
[13]D. K. Tafti and S. P. Vanka, "A numerical study of flow separation and reattachment on a blunt plate," Physics of Fluids A: Fluid Dyamics **3**, 1749–1759 (1991).
[14]L. H. Back and E. J. Roschke, "Shear-layer flow regimes and wave instabilities and reattachment lengths downstream of an abrupt circular channel expansion," Journal of Applied Mechanics, Transactions ASME **39**, 677–681 (1972).
[15]P. Bradshaw and F. Y. Wong, "The reattachment and relaxation of a turbulent shear layer," Journal of Fluid Mechanics **52**, 113–135 (1972).
[16]N. Djilali and I. S. Gartshore, "Turbulent Flow Around a Bluff Rectangular Plate. Part I: Experimental Investigation," Journal of Fluids Engineering **113**, 51–59 (1991).
[17]R. V. Westphal, J. P. Johnston, and J. K. Eaton, "Experimental Study of Flow Reattachment in a Single-Sided Sudden Expansion." NASA Contractor Report 3765 (1984).
[18]M. V. Ötügen, "Expansion ratio effects on the separated shear layer and reattachment downstream of a backward-facing step," Experiments in Fluids **10**, 273–280 (1991).
[19]M. Kiya and K. Sasaki, "Structure of large-scale vortices and unsteady reverse flow in the reattaching zone of a turbulent separation bubble," Journal of Fluid Mechanics **154**, 463–491 (1985).
[20]N. J. Cherry, R. Hillier, and M. E. Latour, "Unsteady measurements in a separated and reattaching flow," Journal of Fluid Mechanics **144**, 13–46 (1984).
[21]M. Yaghoubi and S. Mahmoodi, "Experimental study of turbulent separated and reattached flow over a finite blunt plate," Experimental Thermal and Fluid Science **29**, 105–112 (2004).
[22]K. Mansour and S. Hosseinverdi, "Turbulent Separated-Reattached Flow around a Blunt Flat Plate," in *ICFDP9-EG-284* (2008).
[23]P. J. Saathoff and W. H. Melbourne, "The generation of peak pressures in separated/reattaching flows," Journal of Wind Engineering and Industrial Aerodynamics **32**, 121–134 (1989).
[24]J. P. Stevenson, K. P. Nolan, and E. J. Walsh, "Particle image velocimetry measurements of induced separation at the leading edge of a plate," Journal of Fluid Mechanics **804**, 278–297 (2016).
[25]M. Kiya and K. Sasaki, "Structure of a turbulent separation bubble," Journal of Fluid Mechanics **137**, 83–113 (1983).
[26]V. A. Brederode, *Three-dimensional effects in nominally two -dimensional flows*, Ph.D. thesis, Imperial College of Science and Technology (1974).
[27]Y. Kubo and K. Kato, "The role of end plates in two dimensional wind tunnel tests." Structural Engineering Journal **3**, 179–186 (1986).
[28]H. G. von Kirchhoff, "Zur Theorie freier Flüssigkeitsstrahlen," Journal für Mathematik **LXX**, 289–298 (1868).
[29]A. Roshko, "On the Wake and Drag of Bluff Bodies," Journal of the Aeronautical Sciences **22**, 124–132 (1955).
[30]M. J. Crompton, *The Thin Aerofoil Leading Edge Separation Bubble*, Ph.D. thesis, University of Bristol (2001).
[31]A. Roshko, "On the drag and shedding frequency of two-dimensional bluff bodies," Tech. Rep. July 1954 (National Advisory Committee for Aeronautics, 1954).
[32]S. F. Birch and J. M. Eggers, "A critical review of the experimental data for developed free turbulent shear layers," Tech. Rep. (National Aeronautics and Space Administration, 1973).
[33]F. T. M. Nieuwstadt, B. J. Boersma, and J. Westerweel, "Turbulent Flows," in *Turbulence: Introduction to Theory and Applications of Turbulent Flows* (Springer International Publishing, Cham, 2016) pp. 87–123.
[34]F. H. Champagne, Y. H. Pao, and I. J. Wygnanski, "On the two-dimensional mixing region," Journal of Fluid Mechanics **74**, 209–250 (1976).
[35]C. Fukushima, R. J. Adrian, D. F. G. Durao, M. V. Heitor, M. Maeda, C. Tropea, J. H. Whitelaw, L. Aanen, and J. Westerweel, "Investigation of the mixing process in an axisymmetric turbulent jet using PIV and LIF," in *Laser Techniques for Fluid Mechanics* (Springer Berlin Heidelberg, 2002) pp. 339–356.
[36]I. Wygnanski and H. Fiedler, "Some measurements in the self-preserving jet," Journal of Fluid Mechanics **38**, 577–612 (1969).
[37]B. J. Boersma, G. Brethouwer, and F. T. Nieuwstadt, "A numerical investigation on the effect of the inflow conditions on the self-similar region of a round jet," Physics of Fluids **10**, 899–909 (1998).
[38]H. Blasius, "Grenrschichten in Flussgkeiten mit Kleiner Reibung." Zeitschrift für Angewandte Mathematik und Physik **56**, 1–37 (1908).
[39]M. J. Crompton and R. V. Barrett, "Investigation of the separation bubble formed behind the sharp leading edge of a flat plate at incidence," Proceedings of the Institution of Mechanical Engineers, Part G: Journal of Aerospace Engineering **214**, 157–176 (2000).
[40]D. E. Gault, "An investigation at low speed of the flow over a simulated flat plate at small angles of attack using pitot-static and hot-wire probes," Tech. Rep. (National Advisory Committee for Aeronautics, 1957).
[41]S. Ravi, *RMIT University*, Ph.D. thesis, RMIT University (2011).
[42]H. P. Horton, *Laminar Separation Bubbles in Two and Three Dimensional Incompressible Flow*, Ph.D. thesis, Univertsity of London, Queen Mary College (1968).
[43]D. Oster and I. Wygnanski, "The forced mixing layer between parallel streams," Journal of Fluid Mechanics **123**, 91–130 (1982).
[44]L. M. Rose and J. M. Altman, "Low-speed investigation of the stalling of a thin, faired, double-wedge airfoil with nose flap," Tech. Rep. (National Advisory Committee for Aeronautics, 1950).
[45]R. E. Walraevens and N. A. Cumpsty, "Leading edge separation bubbles on turbomachine blades," ASME International Gas Turbine and Aeroengine Congress and Exposition **1**, 115–125 (1993).
[46]B. K. Hazarika and C. Hirsch, "Behavior of separation bubble and reattached boundary layer around a circular leading edge," in *ASME International Gas Turbine and Aeroengine Congress and Exposition*, Vol. 1 (1994).
[47]L. Tain and N. A. Cumpsty, "Compressor blade leading edges in subsonic compressible flow," Proceedings of the Institution of Mechanical Engineers, Part C: Journal of Mechanical Engineering **214**, 221–242 (2000).
[48]A. V. Arena and T. J. Mueller, "Laminar separation, transition, and turbulent reattachment near the leading edge of airfoils," AIAA Journal **18**, 747–753 (1980).
[49]W. W. Yeung and G. V. Parkinson, "On the steady separated flow around an inclined flat plate," Journal of Fluid Mechanics **333**, 403–413 (1997).
[50]X. I. Yang and C. Meneveau, "Modelling turbulent boundary layer flow over fractal-like multiscale terrain using large-eddy simulations and analytical tools," Philosophical Transactions of the Royal Society A: Mathematical, Physical and Engineering Sciences **375** (2017), 10.1098/rsta.2016.0098.